Published in Engineering Structures 147 (2017) pp. 473-485

Flexural Behavior of Reinforced Concrete Beams Strengthened with Externally Bonded Aluminum Alloy Plates

Hayder A. Rasheed[1]*, Jamal Abdalla[2], Rami Hawileh[2], Adil K. Al-Tamimi[2]

*Corresponding author: Tel. +1(785) 532-1589. Email: hayder@ksu.edu

Abstract

The objective of this experimental investigation is to study the viability and effectiveness of using aluminum alloy (AA) plates as externally bonded flexural reinforcement for reinforced concrete (RC) beams. Ten RC beams were prepared and nine of them were strengthened with externally bonded 2 mm and 3 mm thick AA plates with different mechanical properties. Four strengthened beams had no end wraps or anchorages. Single-layer and double-layer U-wrap CFRP sheets were used in the transverse direction as end anchorages for four strengthened beams and one beam had three double anchorages (two at the ends and one at mid-span). The beams were tested under monotonic load until failure. The goal is to study the effect of using AA plates as externally bonded flexural strengthening material and to explore the effect of end anchorages on the flexural strength and ductility of these beams. The increase in strength over the control unstrengthened specimen ranged from 13% to 40% while the ductility significantly surpassed that of beams strengthened with CFRP sheets. It is observed that the use of end anchorages enhanced the ductility but not the strength of the tested beams. It is also observed that beams without end anchorage failed predominantly in flexure with full de-bonding while beams with end anchorage failed by localized de-bonding and flexure. Furthermore, the performance of the tested beams was compared with numerical predictions by a computer program developed in this study. The results of the numerical models were in close agreement with the measured experimental data. It was concluded that AA plates could be used as an

[1] Professor, Department of Civil Engineering, Kansas State University, Manhattan, KS, USA

[2] Professor, Department of Civil Engineering, American University of Sharjah, Sharjah, UAE

external strengthening material to enhance both the strength and ductility of RC beams in flexure.

Keywords: Aluminum Alloy plates**,** CFRP sheets, flexural strengthening, anchorage, ductility enhancement.

1.0 Introduction

Strengthening and retrofitting of deteriorated and aging building and bridge members is a common practice due to its cost effectiveness nowadays. As a result, various techniques and strengthening materials emerged in the last four decades. Steel and fiber reinforced polymers (FRP) have been used extensively for this purpose as externally bonded reinforcement (EBR). As flexural reinforcement, steel plates and FRP sheets and plates are usually bonded and may be anchored to the soffit of beams to increase the flexural capacity [1-7]. Steel was used as externally bonded/anchored reinforcement material due to its high tensile strength and ductility. However, the susceptibility of steel itself to corrosion and the deterioration of bond strength between steel and concrete due to corrosion made steel plates less attractive to use as EBR. Consequently, FRP emerged and became the dominant EBR material for the last three decades. FRP has superior tensile strength to weight ratio and high resistance to corrosion. However, its brittle rupture and fast degradation under high temperature lead researchers to search for new materials that overcome the shortcomings of steel and FRP. Newly developed aluminum alloys (AA) with high tensile strength and ductility comparable to that of steel, light weight comparable to that of FRP as well as high resistance to corrosion and to high temperature degradation made them viable candidates for externally bonded reinforcement materials [8-11].

The use of steel plates as externally bonded flexural reinforcement material has been investigated by many researchers in the 1980's [1, 12-14]. Motivated by its light weight and corrosion resistance, FRP replaced steel as EBR material for flexural strengthening of concrete members

[3, 15-22]. Other developments in terms of using hybrid CFRP and GFRP strengthening materials to accomplish pseudo ductility have been contributed [23-24]. Guidelines for the design and construction of reinforced concrete members strengthened with externally bonded FRP systems were developed by ACI committee 440 [25]. Specialized textbooks for the design of strengthened reinforced concrete members with FRP started to appear in the literature [26].

In this study, an experimental program is conducted to qualify the viability and potential of using AA plates as EBR strengthening material to reinforced concrete beams. The behavior of AA strengthened beams is tested with and without CFRP sheets acting as end anchorage U-wrap devices. The tensile stress-strain curve of the AA plates is also tested and modeled using analytical formula similar to that of PCI prestressing strand equation [27]. This formula is then incorporated into an interactive nonlinear analysis program to predict the response of RC beams strengthened with AA plates. Comparisons between the experimental and numerical results are also made.

2.0 Experimental Program

2.1 Test Beams

A series of ten RC beams were designed, constructed and tested. The first beam was tested as a control specimen (named CB), see Figure 1. The remaining nine RC beams were strengthened in flexure with AA plates with and without transverse CFRP sheet anchorage systems. Four beams were strengthened without anchorage, two of them using 2 mm thick 5083-0 AA plates (named B1NW and B2NW) and two of them using 3 mm thick 5083-H111 AA plates (named B5NW and B6NW), see Figure 2a. Four other beams, two using 5083-0 plates (named B3SW and B4DW) and two using 5083-H111 plates (named B7SW and B8DW), were anchored with a single and double end U-wraps respectively, see Figure 2b. The last beam specimen was strengthened with 5083-H111 plate and it was anchored with double U-wraps applied at the two ends and at mid-span (named B9TDW), see Figure 2c.

The authors made two identical specimens of each of the beams with no U-Wraps for the sake of repeatability or capturing different failure modes, if any, since this is the first time the behavior of AA strengthened flexural beams is studied. The designation and detail of each beam specimen are also summarized in Table 1.

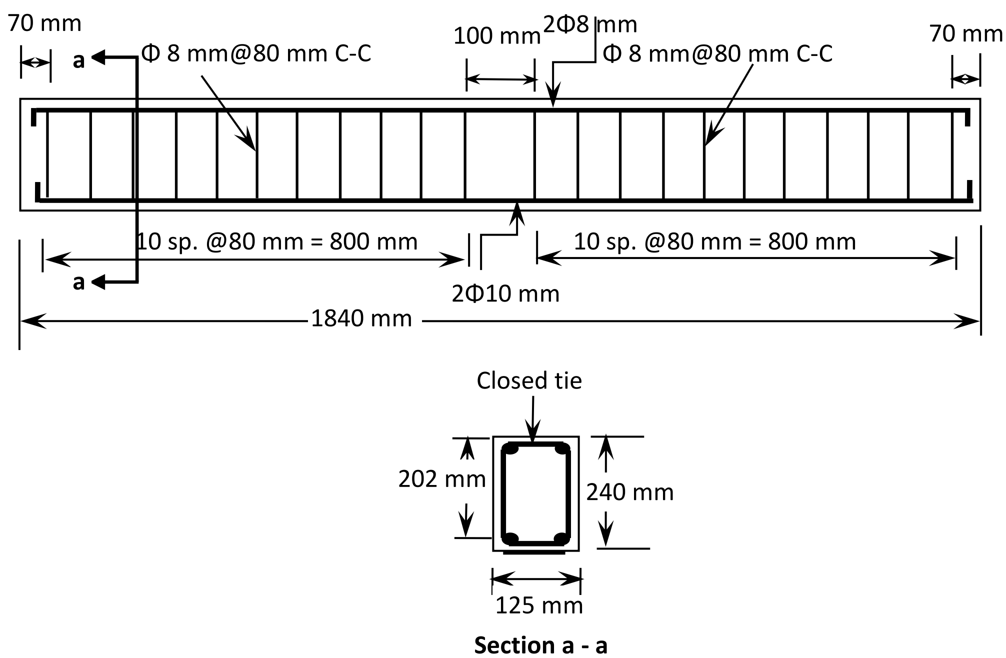

Figure 1 Dimensions and reinforcement details of tested beam

Table 1: Designation and detailing of each beam specimen

designation	AA Plates		Anchorage		
	Thickness: 2mm	Thickness: 3mm	Single U-wraps at the ends	Double U-wraps at the ends	Double U-wraps at the ends and mid-span
CB	-	-	-	-	-
B1NW	√	-	-	-	-
B2NW	√	-	-	-	-
B3SW	√	-	√	-	-
B4DW	√	-	-	√	-
B5NW	-	√	-	-	-
B6NW	-	√	-	-	-
B7SW	-	√	√	-	-
B8DW	-	√	-	√	-

B9TDW	-	√	-	-	√

Each identical beam was 125 mm x 240 mm x 1840 mm in dimensions. The clear span between simple supports was 1690 mm. The beams were reinforced with 2 No. 10 mm bars at the bottom, 2 No. 8 mm bars on top and No. 8 mm stirrups at 80 mm c/c, Figure 1. The AA plates were 1352 mm long by 50 mm wide and 2 mm or 3 mm thick based on the plate type. The width of the CFRP U-wrap sheet was 200 mm, which was applied in the transverse direction in case of the single wrap and in case of the double wrap (90° with the beam axis). The U-wraps anchored the AA plate and were wrapped up to the full height of the beam sides, Figure 2b-c.

Figure 2a Test specimens B1NW, B2NW, B5NW, B6NW

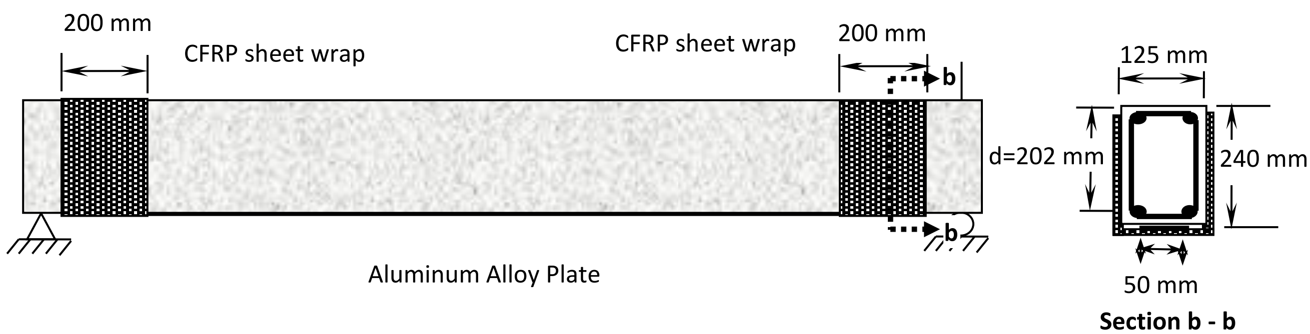

Figure 2b Test specimens B3SW, B4DW, B7SW, B8DW

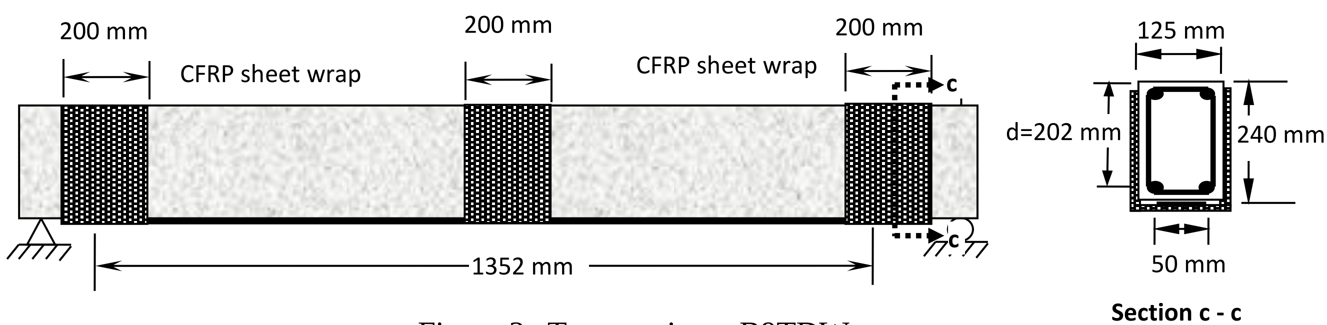

Figure 2c Test specimen B9TDW

Figure 2 Dimensions and detailing of strengthened beam specimens

2.2 Materials

During the casting process, three cylinders were prepared to determine the compressive strength of the concrete mix. The three cylinders were tested at 28 days as shown in Table 2 yielding an average compressive strength of 38.78 MPa. The nominal yield strength of the primary steel reinforcement was reported by the manufacturer to be 550 MPa. Nevertheless, three rebar specimens were tested in the laboratory yielding the results presented in Table 3. The average yield strength was found to be 540.14 MPa, while the average tensile strength was determined to be 640.17 MPa. The average modulus of elasticity came out to be 199.97 GPa. Three specimens of each type of the AA plates used in flexural strengthening were tested in tension in the laboratory. The 5083-0 AA plates with 2 mm thickness have the mechanical properties listed in Table 4. The 5083-H111 AA plates with 3 mm thickness have the mechanical properties listed in Table 5. The experimental stress-strain curves of the two types of plates are shown in Figure 3. The modulus of elasticity of the 5083-0 AA plates was 50,000 MPa. On the other hand, the modulus of Elasticity of the 5083-H111 AA plates was 20,425 MPa. The CFRP U-wrap sheets used were SikaWrap-300C with the following manufacturer properties: thickness of 0.17 mm, tensile strength of 3900 MPa, ultimate strain of 1.5%, and modulus of elasticity of 230 GPa [28].

Sikadur-30LP [29] is the epoxy adhesive used in this study. It is an adhesive used for bonding structural strengthening reinforcements. It has compressive strength, flexural strength and shear strength of 85 MPa, 25 MPa and 17 MPa, respectively. The epoxy used with SikaWrap-300C CFRP sheet is Sikadur-330 [30]. It has a tensile strength of 30 MPa and tensile modulus of elasticity of 4.5 GPa. In terms of thermal resistance, the glass transition temperature (T_G) of Sikadur-30LP and Sikadur-330 is 72 and 82°C, respectively as reported by the manufacturer [29-

30]. Residual epoxy strength beyond these temperatures may exist. However, it is not well-documented in the literature at this point.

Table 2: Concrete cylinder compressive strength testing results

Specimen	Cylinder 1	Cylinder 2	Cylinder 3	**Average**
Compressive Strength (MPa)	35.82	37.17	43.34	**38.78**

Table 3: Coupon test results of steel reinforcement

Specimen	Rebar 1	Rebar 2	Rebar 3	**Average**
Yield Strength (MPa)	538.78	544.35	537.28	**540.14**
Tensile Strength (MPa)	655.05	633.20	632.26	**640.17**
Modulus of Elasticity (GPa)	200.02	199.91	199.99	**199.97**

Table 4: Mechanical Properties of Aluminum Alloy 5083-0

Specimen	F_y (MPa)	F_u (MPa)	Elongation (%)
A1	141	281.87	22.34
A2	150	304.42	23.94
A3	148	292.78	26.71
Average Experimental	146.33	293.03	24.33
Manufacturer	145	295	22

Table 5: Mechanical Properties of Aluminum Alloy 5083-H111.

Specimen	F_y (MPa)	F_u (MPa)	Elongation (%)
S1	135	302.20	35.30
S2	214.03	293.74	29.20
S3	131	308.29	32.20
Average Experimental	160.01	301.41	32.23
Manufacturer	148	288.60	20.90

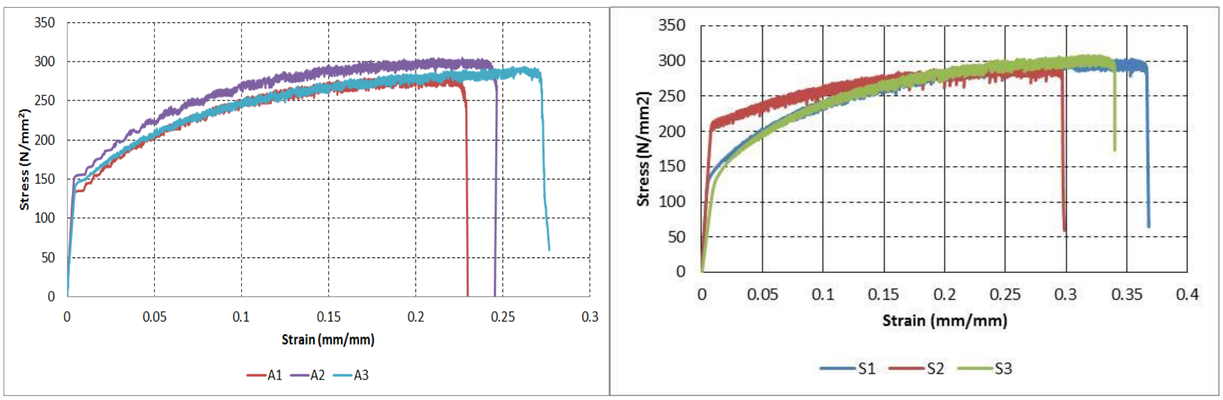

Figure 3 Experimental stress-strain curves for 5083-0 and 5083-H111 AA plates.

2.3 Test Matrix

The control beam (CB) was left un-strengthened, while the remaining 9 beams were strengthened with different AA flexural plates bonded to the soffit of the beams symmetrically about their mid-spans. The AA plate for the B1NW and B2NW specimens was bonded along 80% of the span length (70% of shear span length) to serve as strengthened control specimens for the 5083-0 AA plate, to simulate basic composite action without end anchorage and to represent strengthening RC beams with the current state-of-the-art procedure, Figure 2a. The third strengthened specimen B3SW was identical to the strengthened control specimens in everything except for a single transverse CFRP U-wrap layer at the ends, Figure 2b. The fourth strengthened specimen B4DW was identical to the strengthened control specimens in everything except for double transverse CFRP U-wrap layers at the ends.

The fifth and sixth specimens B5NW, B6NW, serve as strengthened control specimens for the 5083-H111 AA plate to simulate basic composite action without end anchorage as well. The seventh strengthened specimen B7SW was identical to its strengthened control counterparts B5NW and B6NW plus end anchorage identical to that of B3SW. The eighth strengthened specimen B8DW was identical to its strengthened control counterparts B5NW and B6NW plus end anchorage identical to that of B4DW. The ninth strengthened specimen B9TDW was identical to its strengthened control counterparts B5NW and B6NW with three double U-wrap anchorages at the ends as well as the mid span, Figure 2c.

2.4 Experimental Test Setup

The beams were tested under four-point bending monotonically until failure. Displacement control protocol was followed throughout the testing process at a rate of 2 mm/minute. The shear span on each side of the applied load was limited to 561.5 mm while the distance between the two point loads was 567mm, Figure 4. The AA plate covered 80% of the full span which corresponded to 70% of the shear span. Strain gages were applied exactly at mid-span on the concrete top surface and the AA plate in each beam specimen.

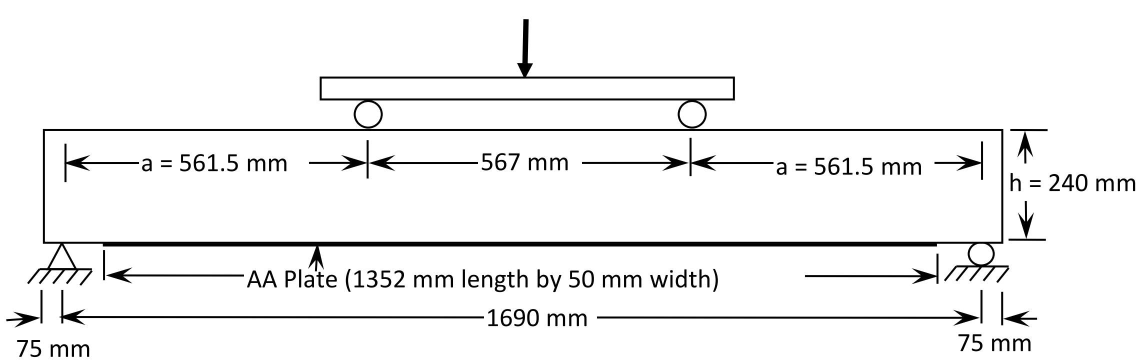

Figure 4 Details of tested beam and location of four points loading

3.0 Numerical Analysis

3.1 Computer Program

An Excel-based interactive nonlinear beam analysis program is developed here to compare the experimental load-deflection response to numerical predictions. The program follows the incremental deformation technique to generate the moment-curvature response, Figure 5. The latter is numerically integrated to yield the load-mid span deflection curve. The program accounts for the nonlinearity of concrete in compression by using the Hognestad's parabola [31]. The stress strain curve of the internal steel reinforcement is assumed to be elastic-perfectly plastic. However, Figure 3 clearly shows that the stress-strain curve of the AA plate is mainly strain hardening that cannot accurately be depicted by an elastic-perfectly plastic curve. Accordingly, the stress-strain curve of the Aluminum Alloy is accurately modeled in the next subsection. Other assumptions that the program makes are:

1. Plane sections before bending remain plane after bending and perpendicular to the mid surface.
2. Concrete in tension after cracking assumes the smeared crack approach and implements the tension stiffening model developed by Nayal and Rasheed (2006) [32].
3. The small strain mismatch between the concrete extreme tension fiber and the AA plate, due to bonding the zero strain plate while the beam is under self-weight, is accounted for in this analysis.
4. The beam half span is divided into a large number of segments to accurately account for the actual variation of stiffness with increasing the load along the beam. Numerical integration is applied to compute the mid-span deflection. The program can divide the beam half span to up to 100 segments. However, 50 segments are found sufficient to accurately predict the deflection.

3.2 AA Constitutive Model

The stress-strain curve of the AA plates is linear at first followed by a strain hardening region according to Figure 3. Therefore, a stress-strain model similar to that of the PCI prestressing strand formula is adopted to capture the AA strain hardening constitutive response. The formula is generally of the following expression:

$$\sigma_{AA} = \sigma^* - \frac{a}{\epsilon_{AA} - b} \qquad (1)$$

Where σ^*, a and b are constants to be recovered from three key representative points along the strain hardening region. To capture a representative stress-strain curve for AA 5083-0, the following three points are selected: Yielding point (0.0030, 150), Ultimate Point (0.2622, 292) and a point in between (0.1354, 262.75). By substituting these three points into Equation (1), the following three parameters are recovered: σ^*= 342.35 MPa, a= 17.372 MPa, b= -0.08285. These parameters yield the stress-strain expressions below, Figure 6:

$$\sigma_{AA} = 50{,}000 \times \epsilon_{AA}, \quad \epsilon_{AA} \leq 0.003 \qquad (2)$$

$$\sigma_{AA} = 342.35 - \frac{17.372}{\epsilon_{AA} + 0.08285}, \qquad \epsilon_{AA} > 0.003 \qquad (3)$$

On the other hand, the representative stress-strain curve for AA 5083-H111 uses the following three points: Yielding point (0.00661, 135.00), Ultimate Point (0.35775, 297.92) and a point in between (0.14839, 262.80). In this case, the yielding point is selected to be different from the average of three specimens in Table 5 since the yielding point of specimen S2 is considered to be an outlier and the average of the other two specimens is considered herein as it happened to be consistent and on the conservative side. By substituting these three points into Equation (1), the following three key parameters are recovered: σ^*= 339.90 MPa, a= 16.809 MPa, b= -0.07369. These parameters yield the stress-strain expressions below, Figure 6:

$$\sigma_{AA} = 20{,}425 \times \epsilon_{AA}, \quad \epsilon_{AA} \leq 0.00661 \tag{4}$$

$$\sigma_{AA} = 339.90 - \frac{16.809}{\epsilon_{AA}+0.07369}, \qquad \epsilon_{AA} > 0.00661 \tag{5}$$

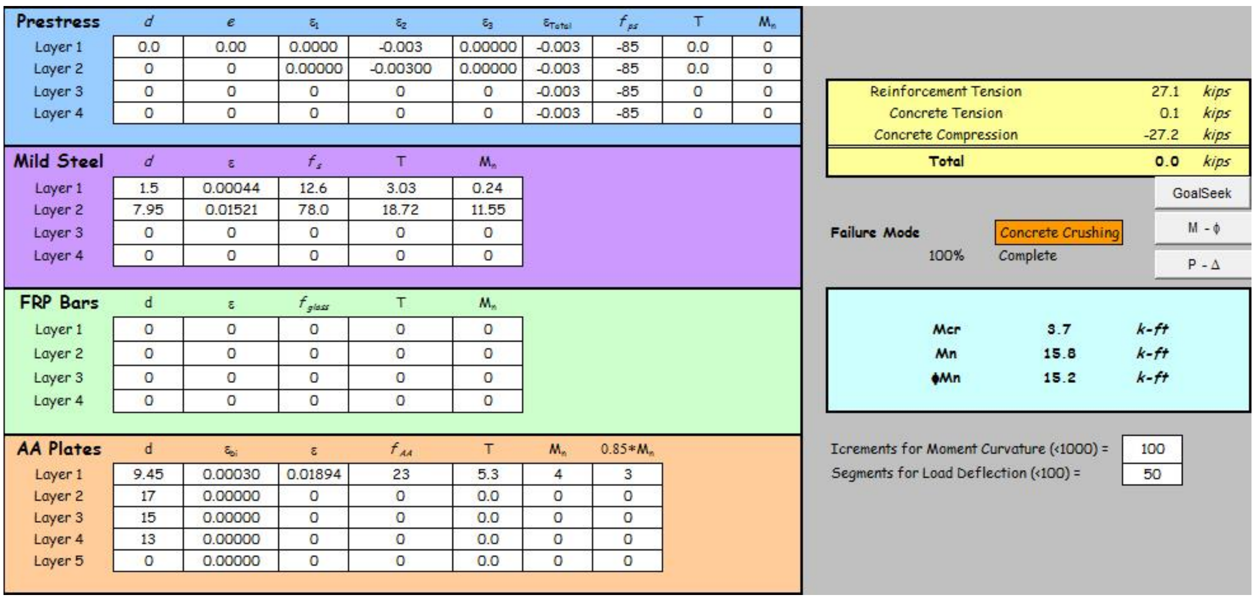

Figure 5 Beam program main control panel.

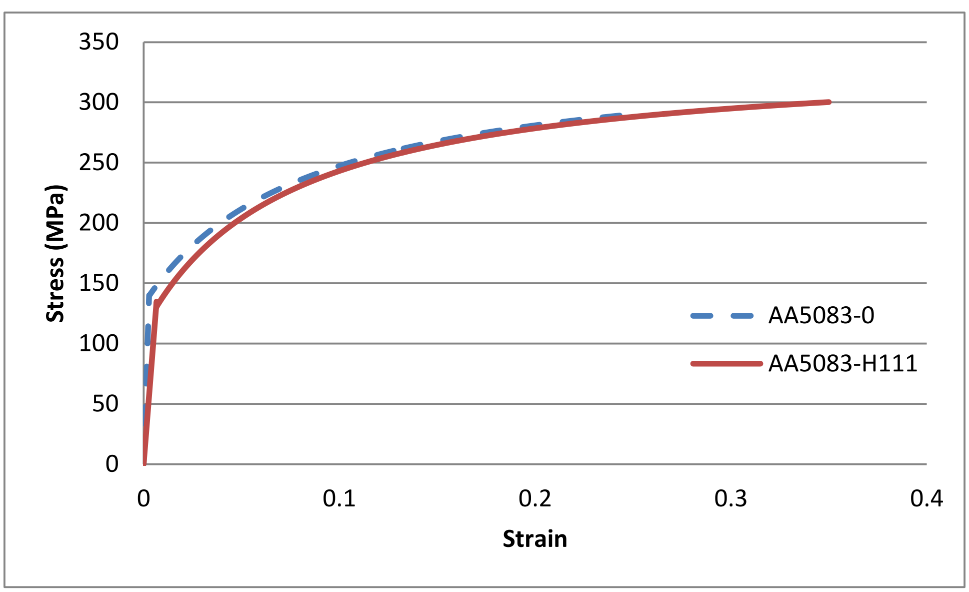

Figure 6 Representative stress-strain models for AA 5083-0 and 5083-H111 plates.

4.0 Results and Discussion

4.1 Summary of loads, deflections and ductility indices

Unlike the strengthening of RC beams with FRP, strengthening with AA plates yield ductile response similar to that of the control beam, see Figure 7. It is also interesting to report that the beams strengthened with AA plates only without end anchorage generally reproduced ductility levels slightly lower than that of the control beam. On the other hand, beams strengthened with AA plates along with end anchorage generally reproduced comparable ductility levels to that of the control beam, Figure 7. Table 6 summarizes the peak loads and the key deflection parameter defined as the deflection at first yield (δ_y), the deflection at peak load (δ_u) and the deflection at failure (δ_f). The deflection at first yield represents the mid-span yielding of the internal reinforcement for the control beam and the mid span yielding of the AA plate for the strengthened beams. The deflection at failure represents the complete de-bonding of the AA plate in case of beams with no anchors and locally in between the U-wraps for anchored beams. It is evident that the beams strengthened with 5083-0 AA plates have higher peak loads with end anchorage compared to those without end anchorage. The opposite is true for the beams strengthened with 5083-H111 AA plates. Those with no end anchorage failed at noticeably higher loads than those with end anchorage. This may be attributed to the variation in the yielding strength of the same type of AA plates which is not affected by the anchorage provided, Tables 4-5. It may also be observed from Table 6 that the deflection corresponding to the peak load of strengthened beams took place at a lower mid span deflection than that of the control beam. However, the deflection when the load dropped off for the strengthened beams with double wraps always exceeded that of the control beam. It may also be indicative in this application to report the ductility index values for all the strengthened specimens compared to

299 the control beam since all beams have distinct yielding point in their load-deflection response,

300 Table 7.

301 Table 6 Summary of ultimate loads and deflections

Specimen	P_u (kN)	% P_u Increase over CB	δ_y (mm)	δ_u (mm)	% δ_u Decrease over CB	δ_f (mm)	% δ_f Increase over CB
CB	58.78	-	9.36	32.74	-	33.75	-
B1NW	67.78	15.31	7.13	28.19	-13.90	34.75	2.96
B2NW	66.57	13.25	6.23	22.85	-30.21	27.08	-19.76
B3SW	73.37	24.82	6.15	20.44	-37.57	34.53	2.31
B4DW	71.38	21.44	7.18	48.15	47.07	48.15	42.67
B5NW	82.31	40.03	7.20	25.16	-23.15	25.92	-23.20
B6NW	81.23	38.28	7.38	24.00	-26.70	28.43	-15.76
B7SW	75.95	29.21	6.65	21.37	-34.73	29.55	-12.44
B8DW	74.19	26.22	6.82	24.71	-24.53	37.56	11.29
B9TDW	74.30	26.40	7.54	23.11	-29.41	30.57	-9.42

302

303 Table 7 Summary of ductility indices at ultimate and failure loads

Specimen	δ_y (mm)	δ_u (mm)	δ_f (mm)	$\mu_{\Delta,\,ult}$	Ratio of $\mu_{\Delta,\,ult}$ to CB	$\mu_{\Delta,\,fail}$	Ratio of $\mu_{\Delta,\,fail}$ to CB
CB	9.36	32.74	33.75	3.50	1.00	3.61	1.00
B1NW	7.13	28.19	34.75	3.95	1.13	4.87	1.35
B2NW	6.23	22.85	27.08	3.67	1.05	4.35	1.21
B3SW	6.15	20.44	34.53	3.32	0.95	5.61	1.56
B4DW	7.18	48.15	48.15	6.71	1.92	6.71	1.86
B5NW	7.20	25.16	25.92	3.49	1.00	3.60	1.00
B6NW	7.38	24.00	28.43	3.25	0.93	3.85	1.07
B7SW	6.65	21.37	29.55	3.21	0.92	4.44	1.23
B8DW	6.82	24.71	37.56	3.62	1.04	5.51	1.53
B9TDW	7.54	23.11	30.57	3.06	0.88	4.05	1.12

304

305 ***4.2 Load-deflection curve***

306 The load-deflection curves of identical beams are seen to be perfectly matching except at
307 ultimate failure. It can be seen from Figure 7a that the load-deflection response of beams B1NW
308 and B2NW are identical until reaching the peak load of B2NW at a mid-span deflection of

around 23 mm. After that point, the response of B1NW continues to slightly increase until a deflection of 28 mm while the response of B2NW gradually declines. The same observation can be made regarding the response of beams B5NW and B6NW without end anchorage, Figure 7c. The response of the beams with end anchorage is shown to follow a similar trend while the beams having double anchorage B4DW and B8DW experience significantly more ductility than those with single anchorage B3SW and B7SW, Figure 7b and d.

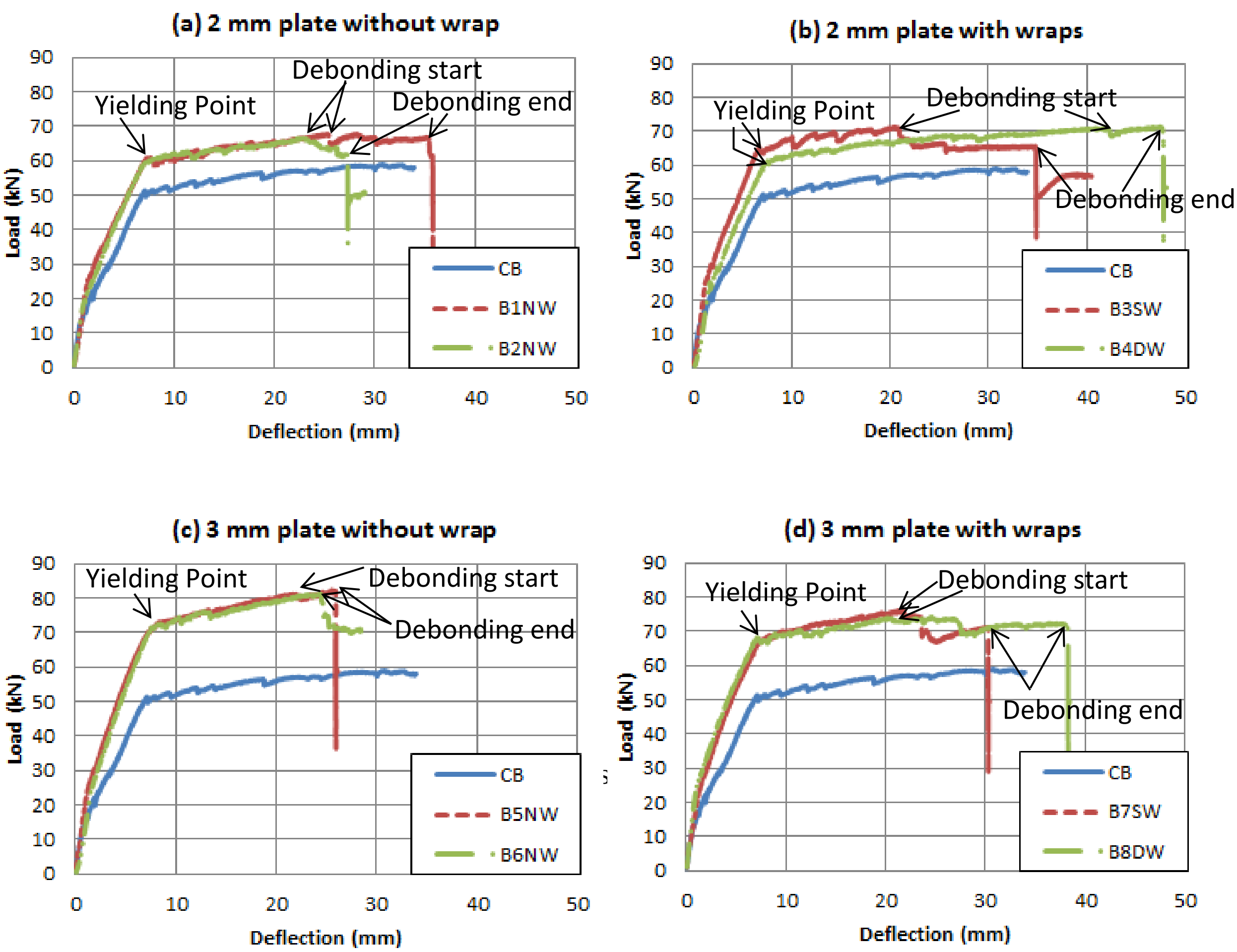

Figure 7 Load-deflection for beams with and without wraps

Surprisingly enough, the ductility presented by the last beam B9TDW having the extra mid-span anchorage was the lowest, Figure 8. This may be attributed to the fact that the AA plate in that beam completely de-bonded in between the end and mid-span U-wraps and buckled outward early on after steel yielding, see Figure 14. The remedy to this behavior may be to provide equally-spaced distributed U-wraps along the shear span as done by Rasheed et al. [3]. Since all the beams were loaded in displacement control and since the end of the de-bonding stage renders the AA plate completely separate from the beam, an abrupt vertical drop in the load deflection curve takes place at the point of loss of AA plate where the beam reverts back to the response of the control specimen. In addition to the load-deflection curves, plots of load-strain response in the concrete extreme compression fiber and the AA plates are presented in Figure 9. It is evident that the strain gages on the AA plates have captured and confirmed their yielding plateau.

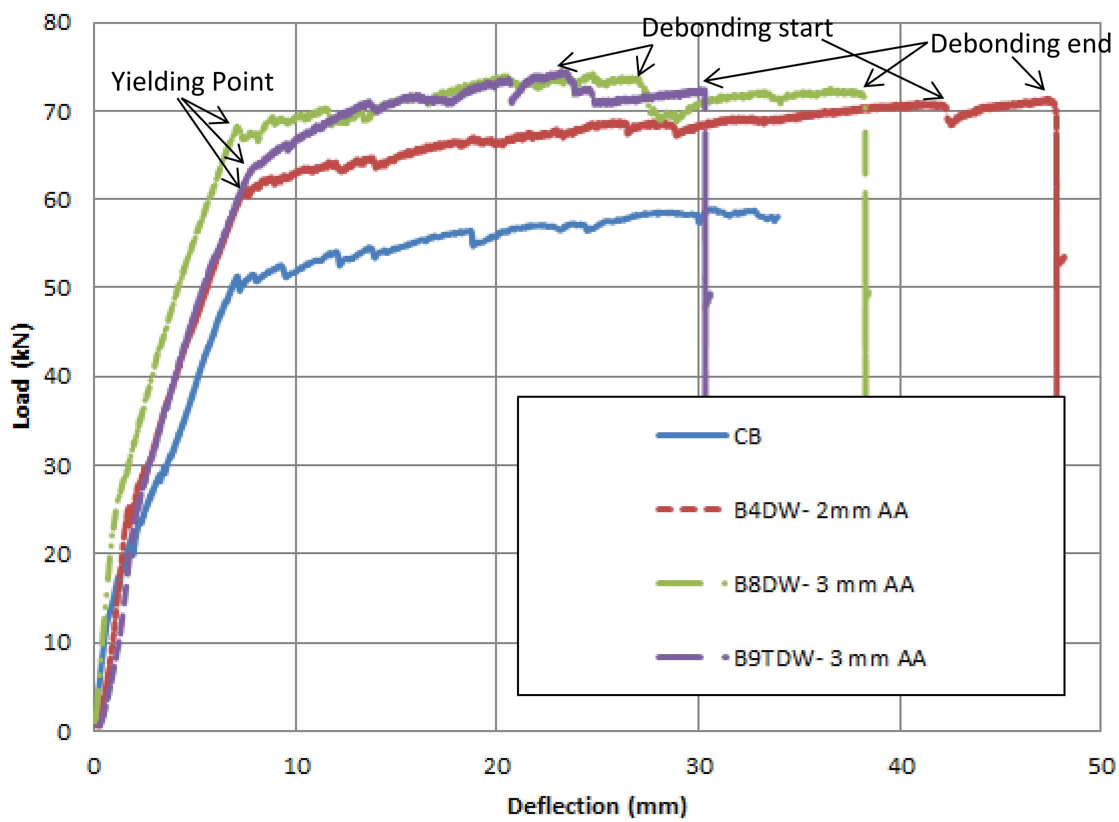

Figure 8 Load-deflection for beams with double-layer end-wraps and triple wraps

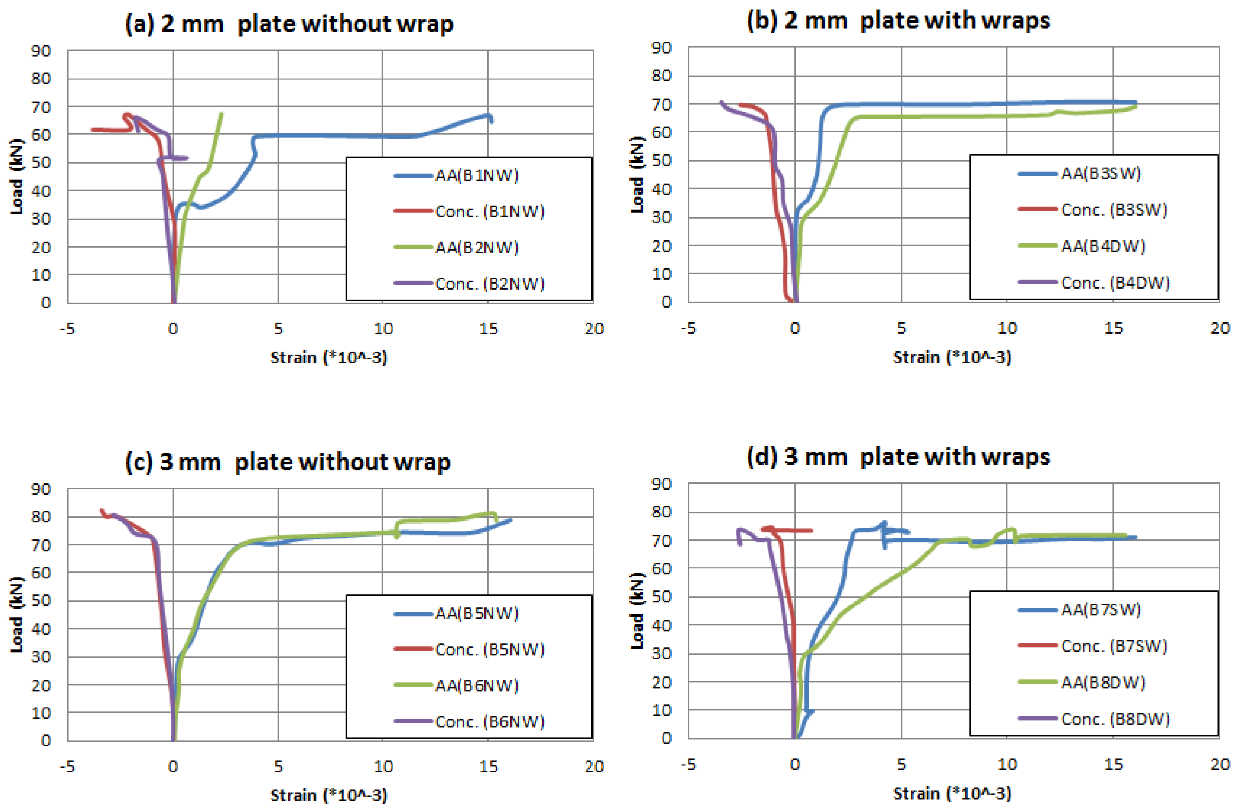

Figure 9 Load-strain for AA and concrete in beams with and without anchorage

4.3 Modes of failure of tested beams

The major role that anchorage played in realizing the failure mode is that beams with no anchorage failed by yielding of the AA plate followed by complete debonding of the AA plate while beams with end anchorage also failed by yielding of the AA plates followed by localized debonding of the AA plate in between the anchors, Table 8. Accordingly, the anchors acted in prolonging the deformation before failure by maintaining the AA plate partially attached to the beams passed the debonding strain level, Figure 7. This is different from the case of FRP strengthened beams in which end anchorage improves the ultimate strength while it only prolongs the overall deformation in case of AA strengthened beams, Figure 10. The comparison in Figure 10 of the CFRP strengthened beam is taken from an earlier study conducted by the authors [24]. The beam's (specimen BC) overall dimensions and span are exactly the same as the present specimens. Nevertheless, the only difference is the EA of the strengthening layer, which is why the load is normalized by EA of the strengthening layer in Figure 10. Figure 11 shows the flexural failure of the beams strengthened with the 5083-0 AA plate. Figure 12 compares the beam deformation at failure between the two beams strengthened with 5083-0 and the two strengthened with 5083-H111 AA plates without end anchorage. Figure 13, on the other hand, presents a similar comparison between the strengthened beams having single and double end anchorage. Figure 14 presents the localized debonding in between the U-wraps upon failure of B9TDW beam with double anchorage at the end and mid-span.

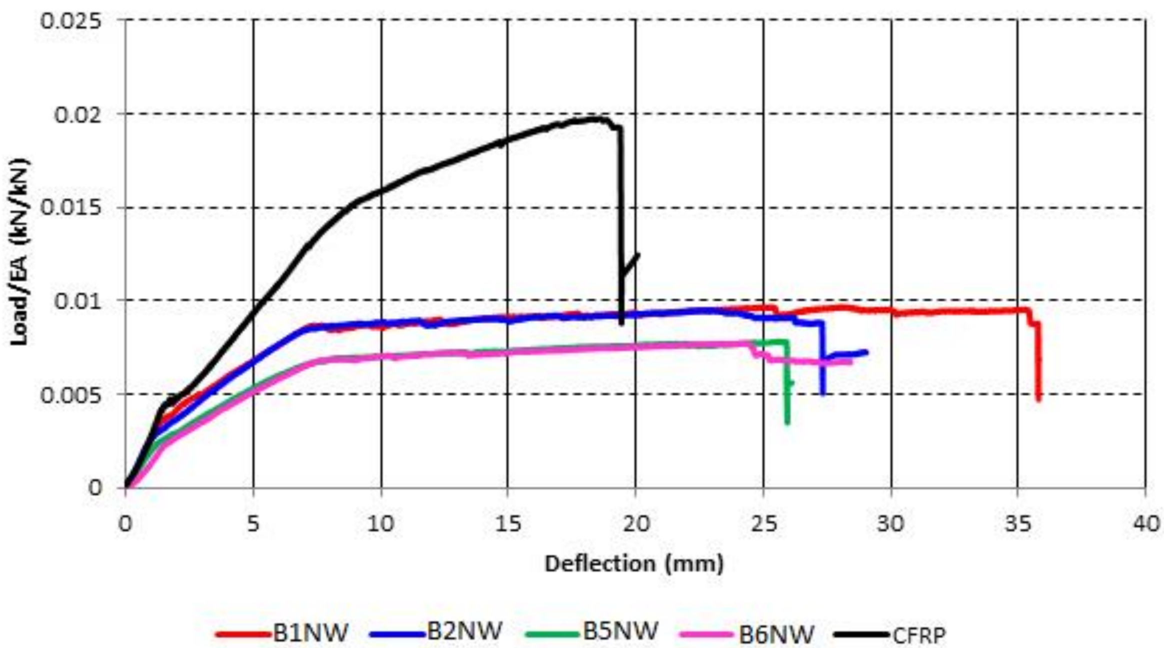

Figure 10 Comparison of load/axial stiffness ratio vs. deflection of AA and CFRP strengthened beams

Table 8 Summary of ultimate loads and failure modes

Specimen	P_u (kN)	Mode of Failure
CB	58.78	Flexural failure
B1NW	67.78	Plate debonding and flexural failure
B2NW	66.57	Plate debonding and flexural failure
B3SW	73.37	Localized debonding and flexural failure
B4DW	71.38	Localized debonding and flexural failure
B5NW	82.31	Plate debonding and flexural failure
B6NW	81.28	Plate debonding and flexural failure
B7SW	75.95	Localized debonding and flexural failure
B8DW	74.19	Localized debonding and flexural failure
B9TDW	74.30	Localized debonding and flexural failure

(a) Control Beam (CB) at failure

(b) Delamination failure of B1NW

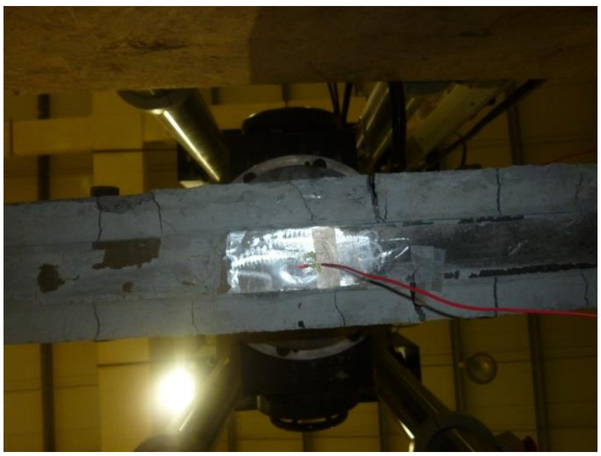

(c) Flexure failure of B2NW

(d) B4DW ready for test

Figure 11 Failure modes of different beams

(a) B1NW Beam at failure

(b) B2NW Beam at Failure

(c) B5NW Beam at failure

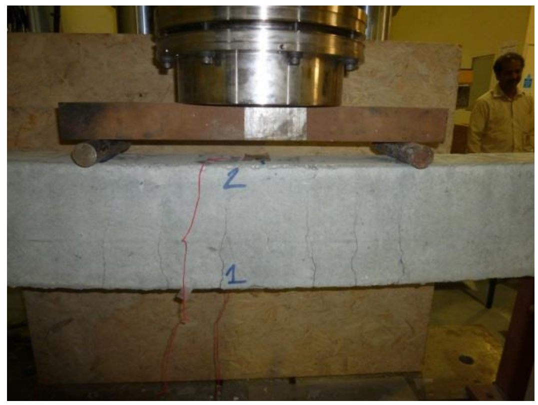

(d) B6NW Beam at failure

Figure 12 Failure modes of un-wraped beams at failure

(a) B3SW Beam at failure

(b) B4DW Beam at Failure

(c) B7SW Beam at Failure

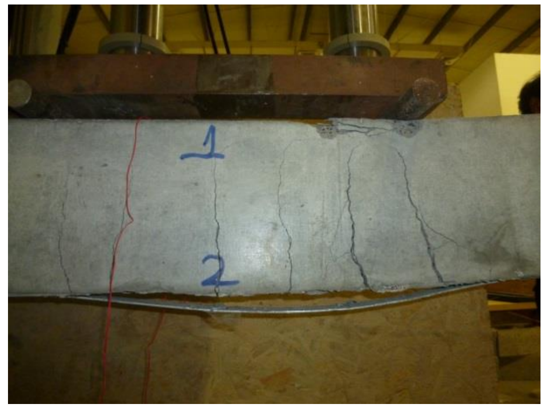

(d) B8DW Beam at Failure

Figure 13 Failure modes of single and double layers end-wraped beams at failure

(a) B9TDW Beam at initiation of failure

(b) B9TDW Beam at Failure

Figure 14 Failure modes of double wraped beams in three locations at failure

5.0 Analytical Prediction of Flexural Behavior of AA Strengthened Beams

Using the numerical analysis program developed in section 3.0 above, the prediction of ultimate load for the control beam was found to be 57.72 kN, which is very close to the test result of

58.78 kN, Table 9. In predicting the ultimate debonding load of the AA strengthened beams without anchorage, the debonding strain formula presented by ACI 440.2R-08 [25] for FRP sheets is used here by replacing the strengthening material properties with those of the AA plate:

$$\varepsilon_{fd} = 0.41\sqrt{\frac{\acute{f}_c}{nE_f t_f}} \tag{6}$$

$$\varepsilon_{AA5083-0-d} = 0.41\sqrt{\frac{38.78}{1\times 50{,}000\times 2}} = 0.008074 \tag{7}$$

The strain in equation (7) above corresponds to an ultimate load of 68.32 kN which is in excellent agreement with the test values of B1NW and B2NW, Table 9. On the other hand, the anchored beams are treated as capable of achieving flexural failure by concrete crushing with a top concrete strain of 0.003. This corresponds to an ultimate load of 70.52kN, which is slightly lower than the test results of B3SW and B4DW beams.

Similarly, the beams strengthened with the thicker AA plate (5083-H111) are estimated to have a debonding strain of:

$$\varepsilon_{AA5083-H111-d} = 0.41\sqrt{\frac{38.78}{1\times 20{,}425\times 3}} = 0.01031 \tag{8}$$

This strain in equation (8) above corresponds to an ultimate load of 73.33 kN which is in noticeably lower than the ultimate loads of beams B5NW and B6NW, Table 9. This may be attributed to the fact that these two beams might have had a plate with higher values than the average properties used in the analysis (e.g. Specimen S2 of Table 4). On the other hand, the anchored beams were treated as capable of achieving flexural failure by concrete crushing with a top concrete strain of 0.003. This corresponds to an ultimate load of 75.27kN, which is in excellent agreement with the last three anchored beams B7SW, B8DW and B9TDW.

Table 9 comparison of analytical ultimate load capacity prediction with experimental results

Specimen	$P_{u, exp}$ (kN)	$P_{u, pred}$ (kN)	Load ratio ($P_{u, pred}$ / $P_{u, exp}$)
CB	58.78	57.72	0.98
B1UW	67.78	68.32	1.01
B2UW	66.57	68.32	1.03
B3SW	73.37	70.52	0.96
B4DW	71.38	70.52	0.99
B5UW	82.31	73.33	0.89
B6UW	81.28	73.33	0.90
B7SW	75.95	75.27	0.99
B8DW	74.19	75.27	1.01
B9TW	74.30	75.27	1.01

6.0 Comparison of Experimental Results and Analytical Predictions

To illustrate the overall comparison of the load-deflection response of the tested beams and the analysis predictions, these two responses are plotted in a graph for each one of the control beam, Beam B1NW/B3SW and B5NW/B7SW. The load-deflection response of the rest of the beams is not shown to avoid repetition and avoid over-crowding the plots with curves that might render the comparison confusing. In Figure 15, the analysis prediction of the control beam compares well with the experimental curve even though the latter shows softer overall response. Figure 16 presents an excellent matching comparison between the analysis and experimental curves up to the point of yield load and corresponding deflection. After that, the analysis curve matches the response of Beam B3SW closely while the response of Beam B1NW is shown to be parallel to the other two curves but yielding at a slightly lower load. Similarly, Figure 17 shows the excellent comparison between the curves of beam B7SW and the analytical prediction all the way to the ultimate load. On the other hand, the response of Beam B5NW is shown to be parallel to the other two curves but yielding at a slightly higher load. This is to be expected due to the small variability in the yield strength of the AA plate coupons tested and presented in this paper.

To present the analytical and experimental load-strain comparison, Figures 18 and 19 are plotted for the beams strengthened with 2 mm AA plate with and without wraps, respectively. It is evident from Figure 18 that the AA strain in Beam B1NW was measured in a direct proximity to a flexural crack while that of Beam B2NW was away from a flexural crack but that strain gage clearly stopped working around the first yield point. The load-strain curves of the concrete top strain shows good correspondence to the analysis values. On the other hand, Figure 19 shows excellent comparison between the strains measured at mid-span in Beams B3SW and B4DW and the predicted values. Furthermore, Figures 20 and 21 show excellent comparisons of the load-strain response on the extreme compression fiber and the AA plate for beams B5NW, B6NW, B7SW and B8DW along with the analytical predictions. It may be observed that the AA plate experimental strains at the critical section at mid-span depend on the proximity to a major flexural crack. However, they are generally reproducible by the present analysis program.

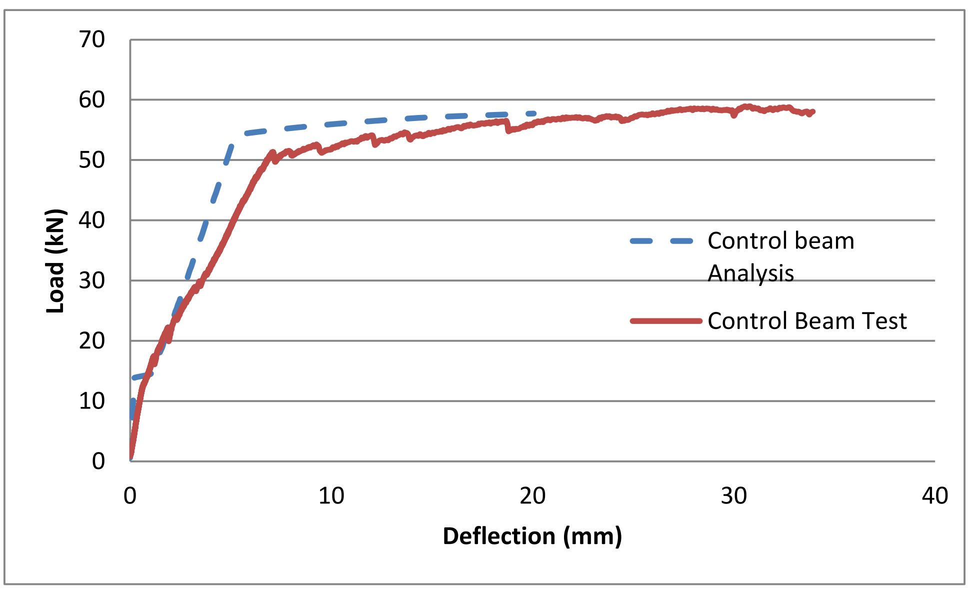

Figure 15 Load-deflection response comparison of the control beam and the analysis prediction

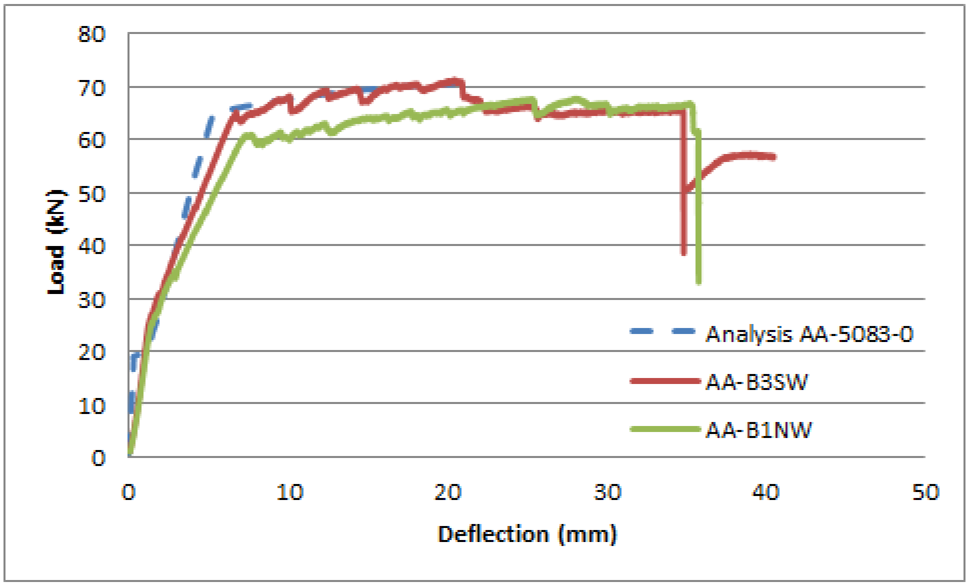

Figure 16 Load-deflection response comparison of the B1NW, B3SW beams and the analysis prediction

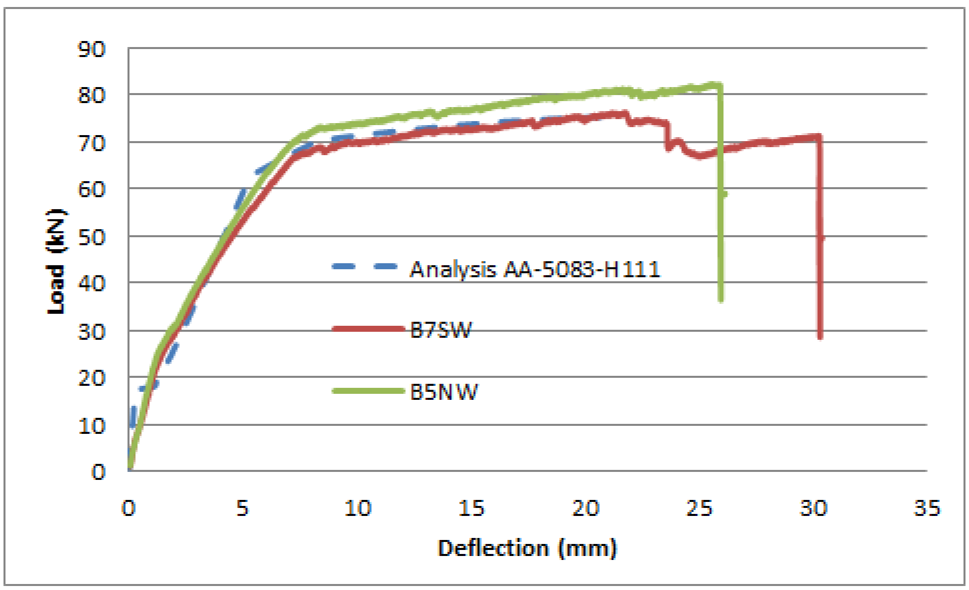

Figure 17 Load-deflection response comparison of the B5NW, B7SW beams and the analysis prediction

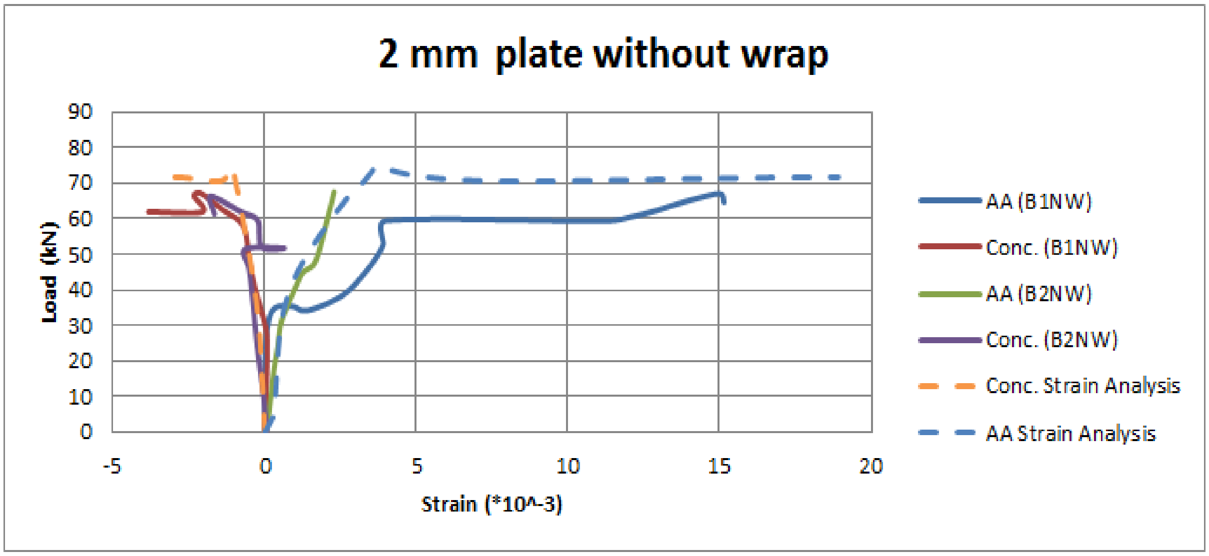

Figure 18 Load-strain response comparison of the B1NW and B2NW beams and the analysis predictions

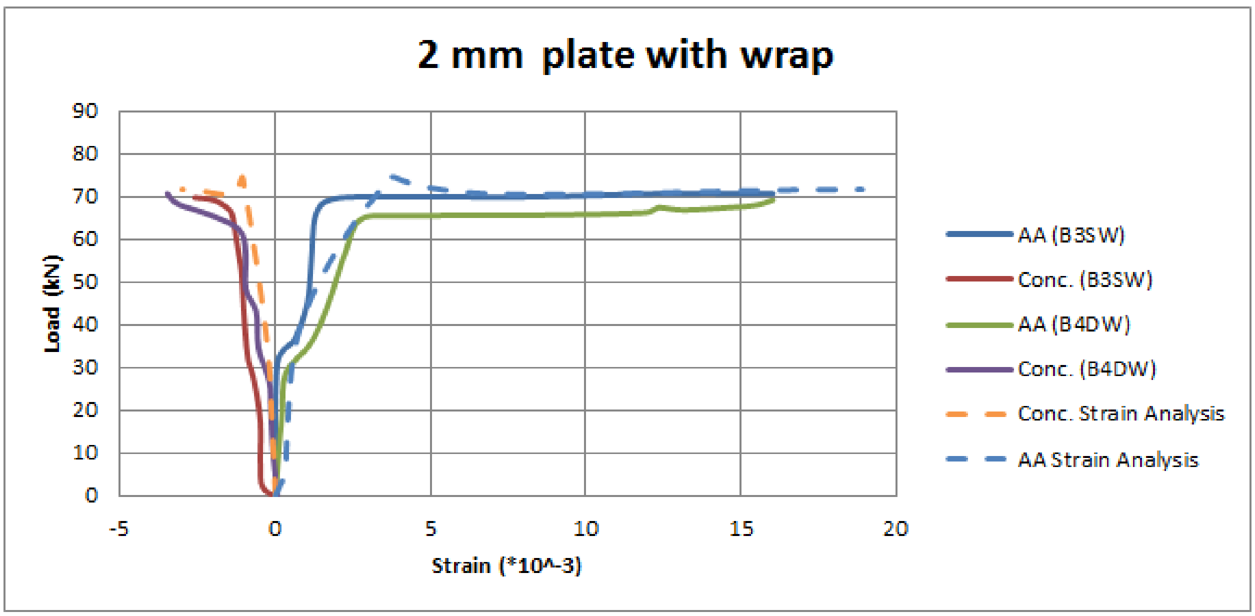

Figure 19 Load-strain response comparison of the B3SW and B4DW beams and the analysis predictions

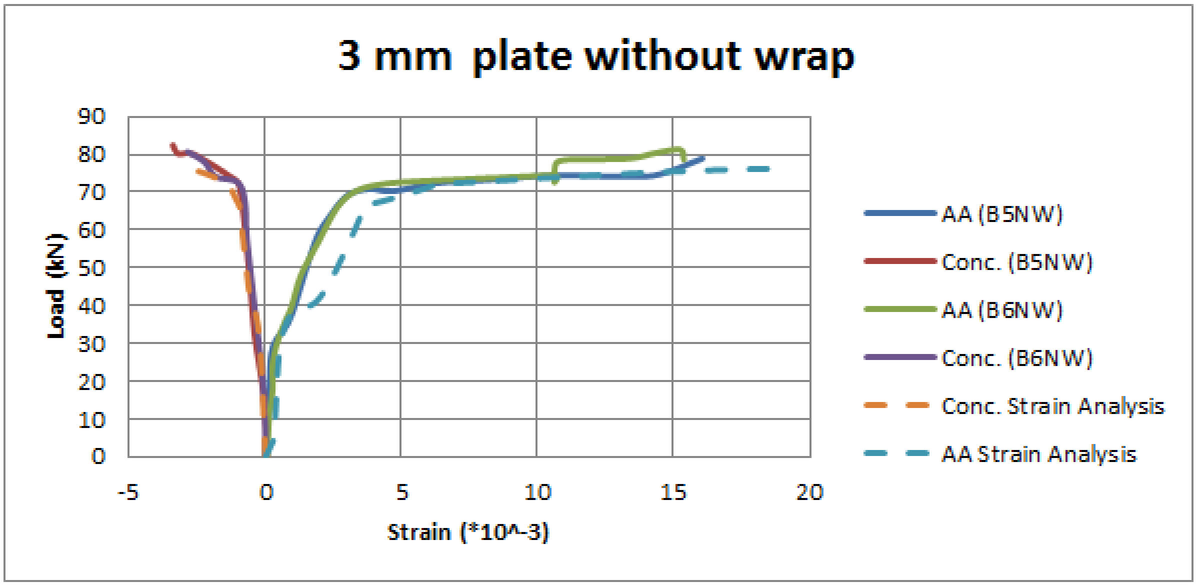

Figure 20 Load-strain response comparison of the B5NW and B6NW beams and the analysis predictions

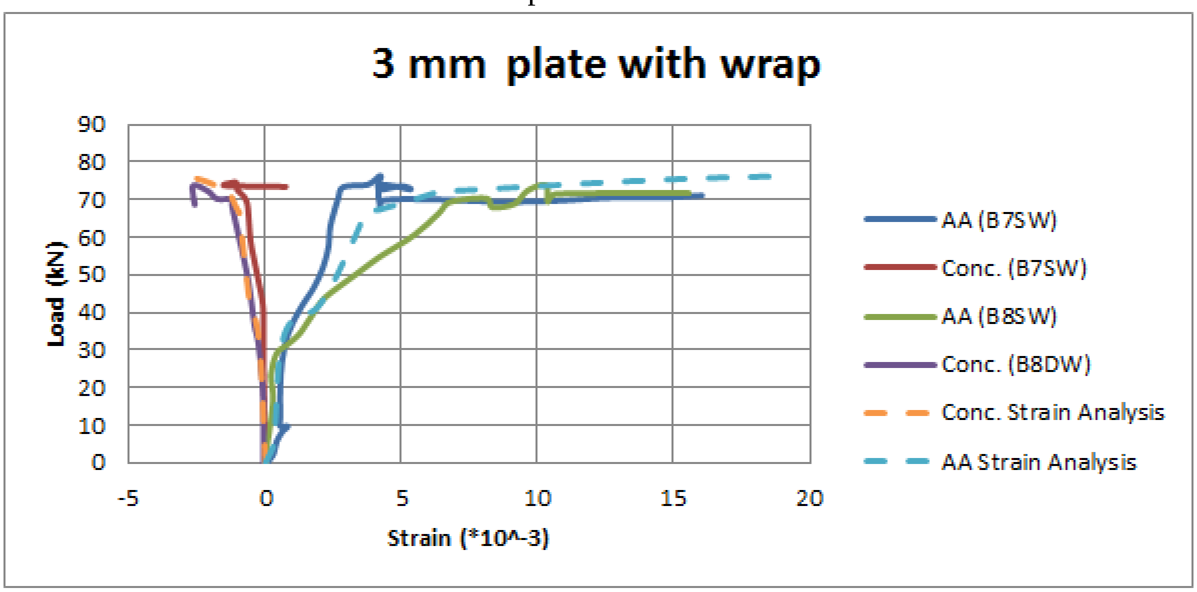

Figure 21 Load-strain response comparison of the B7SW and B8DW beams and the analysis predictions

7.0 Summary and Conclusions

This study introduces for the first time the use of Aluminum Alloy plates as a potential replacement to externally bonded flexural reinforcement made of steel and FRP. However, more direct comparisons are warranted to solidify this claim. An experimental program is conducted to examine the viability and potential of this proposal. One control beam and nine AA strengthened beams were tested monotonically to failure after bonding two different Aluminum Alloy plates to their tension face. The behavior proved to be superior to that of FRP due to the ductility provided. The behavior, on the long run, is expected to be superior to that of steel due to the corrosion resistance of the AA plates. The use of end anchorage in this application proved to provide comparable levels of ductility to that observed for the control beam since it extended the deformation beyond the nominal debonding strain values. On the other hand, the use of end anchorage did not improve the overall strength of the strengthened system due to the flat plateau experienced by yielding of the AA plates. A numerical analysis program is also developed to qualify the experimental results obtained. A strain hardening constitutive model is applied to capture the stress-strain curves of the AA plates. This model is incorporated in the nonlinear beam analysis program to predict the response of reinforced concrete beams strengthened with AA plates. The analytical predictions are found to agree with the test results in an excellent manner for both the global and localized response. The debonding strain formula adopted by ACI 440.2R-08 [25] is found to apply very accurately to predict the debonding strain of the AA strengthened beams with no end anchorage.

8.0 Acknowledgement

The first author is grateful to the Emirates Foundation that provided him with travel support to visit the UAE and help establish this experimental program in 2009.

9.0 References (Harvard Style Using Google Scholar)

1. Jones, R., Swamy, R.N. and Charif, A., 1988. Plate separation and anchorage of reinforced concrete beams strengthened by epoxy-bonded steel plates. *Structural Engineer*, 66(5), pp. 85-94.

2. Al-Tamimi, A.K., Hawileh, R., Abdalla, J. and Rasheed, H.A., 2011. Effects of ratio of CFRP plate length to shear span and end anchorage on flexural behavior of SCC RC beams. *Journal of Composites for Construction*, 15(6), pp.908-919.
3. Rasheed, H.A., Decker, B.R., Esmaeily, A., Peterman, R.J. and Melhem, H.G., 2015. The Influence of CFRP Anchorage on Achieving Sectional Flexural Capacity of Strengthened Concrete Beams. *Fibers*, 3(4), pp.539-559.
4. Ali, A. Abdalla, J.A., Hawileh, R.A., Galal, K. 2014. CFRP mechanical anchorage for externally strengthened RC beams under flexure. Physics Procedia 55, pp. 10-16.
5. Spadea, G., Bencardino, F., Sorrenti, F., Swamy, R.N., 2015. Structural effectiveness of FRP materials in strengthening RC beams. Engineering Structures, 99(15), pp. 631-641.
6. Esfahani, M.R.. Kianoush, M.R., Tajari, A.R. 2007. Flexural behaviour of reinforced concrete beams strengthened by CFRP sheets. Engineering Structures, 29(10), pp. 2428-2444.
7. Kotynia, R. and Cholostiakow, S. 2015. New Proposal for Flexural Strengthening of Reinforced Concrete Beams Using CFRP T-Shaped Profiles. Polymers, Volume 7, pp. 2461-2477.
8. Abdalla, J. A., Abu-Obeidah, A. and Hawileh, R. A. 2011. Behavior of Shear Deficient Reinforced Concrete Beams with Externally Bonded Aluminum Alloy Plates. *The 2011 World Congress on Advances in Structural Engineering and Mechanics (ASEM\'11+ Congress*, Seoul, South Korea, September 18- 23.
9. Abu-Obeidah, A., Hawileh, R.A. and Abdalla, J.A., 2015. Finite element analysis of strengthened RC beams in shear with aluminum plates. *Computers & Structures*, 147(5), pp.36-46.
10. Abdalla, J.A., Abu-Obeidah, A.S, Hawileh, R.A., Rasheed, H.A., 2016. Shear strengthening of reinforced concrete beams using externally-bonded aluminum alloy plates: An experimental study. Construction and Building Materials 128, pp. 24-37.
11. Abdalla, J.A., Hraib, F.H., Hawileh, R.A., Mirghani, A.M., 2017. Experimental investigation of bond-slip behavior of aluminum plates adhesively bonded to concrete. Journal of Adhesion Science and Technology, 31(1), pp. 82-99.
12. MacDonald, M.D. and Calder, A.J.J., 1982. Bonded steel plating for strengthening concrete structures. *International Journal of Adhesion and Adhesives*, 2(2), pp.119-127.

13. Swamy, R.N., Jones, R. and Bloxham, J.W., 1987. Structural behaviour of reinforced concrete beams strengthened by epoxy-bonded steel plates. *Structural Engineer*. Part A, 65, pp.59-68.
14. Roberts, T.M. and Hajikazemi, H., 1989. Theoretical study of the behaviour of reinforced concrete beams strengthened by externally bonded steel plates. *Proceedings of the Institution of Civil Engineers*, 87(1), pp.39-55.
15. Naser, M.Z., Hawileh, R.A., Abdalla, J.A., Al-Tamimi, A.K., 2012. Bond behavior of CFRP cured laminates: experimental and numerical investigation. *Journal of Engineering Materials and Technology*, 134(2), 021002, 9 pages, doi:10.1115/1.4003565.
16. Al-Tamimi,A.K. Hawileh, R.A., Abdalla, J.A., Rasheed, H.A., Al-Mahaidi, R., 2014. Durability of the bond between CFRP plates and concrete exposed to harsh environments. *Journal of Materials in Civil Engineering*, 27(9), 04014252.
17. Meier, U., 1995. Strengthening of structures using carbon fibre/epoxy composites. *Construction and Building Materials*, *9*(6), pp.341-351.
18. Saadatmanesh, H. and Ehsani, M.R., 1991. RC beams strengthened with GFRP plates. I: Experimental study. *Journal of Structural Engineering*, *117*(11), pp.3417-3433.
19. Chajes, M.J., Thomson, T.A., Januszka, T.F. and Finch, W.W., 1994. Flexural strengthening of concrete beams using externally bonded composite materials. *Construction and Building Materials*, *8*(3), pp.191-201.
20. Täljsten, B., 1997. Strengthening of beams by plate bonding. *Journal of materials in civil engineering*, *9*(4), pp.206-212.
21. Rahimi, H. and Hutchinson, A., 2001. Concrete beams strengthened with externally bonded FRP plates. *Journal of composites for construction*, *5*(1), pp.44-56.
22. Kotynia, R., Abdel Baky, H., Neale, K. W., & Ebead, U. A. (2008). Flexural strengthening of RC beams with externally bonded CFRP systems: Test results and 3D nonlinear FE analysis. *Journal of Composites for Construction*, 12(2), 190-201.
23. Grace N, Abdel-Sayed G, Ragheb W. (2002) “Strengthening of concrete beams using innovative ductile fiber-reinforced polymer fabric,” ACI Struct J 2002; 99(5), 692-700.
24. Hawileh, R.A., Rasheed, H.A., Abdalla, J. and Al-Tamimi, A. K. (2014) “Behavior of Reinforced Concrete Beams Strengthened with Externally Bonded Hybrid Fiber Reinforced Polymer Systems,” ***Materials and Design***, Vol. 53, Jan. 2014, pp. 972-982.

25. American Concrete Institute (ACI). (2008). Guide for the design and construction of externally bonded FRP systems for strengthening concrete structures. *ACI No. 440.2R-08*, Farmington Hills, Mich.
26. Rasheed, H. A., (2015) "Strengthening Design of Reinforced Concrete with FRP," CRC Press, 230 p.
27. PCI Design Handbook (2004) "Precast and Prestressed Concrete Design Handbook," 6th edition, Precast/Prestressed Concrete Institute, p. 11-32.
28. Sika Schweiz AG, (2003). *SikaWrap-300: Carbon Fiber Fabric for Structural Strengthening*. Product Data Sheet, Sika Construction Chemicals.
29. Sika Product Data Sheet (2006). *Sikadur-30 LP*: *Two-Part Epoxy Adhesive for bonding reinforcement,* Sika Construction Chemicals.
30. Sika Product Data Sheet, (2009). *Sikadur-330: Two-Part Epoxy Impregnation Resin*. Sika Construction Chemicals.
31. Hognestad, E. 1951. A study of combined bending and axial load in reinforced concrete members, University of Illinois Engineering experiment Station Bulletin No. 399. November 1951, 128p.
32. Nayal, R. and Rasheed, H.A., 2006. Tension stiffening model for concrete beams reinforced with steel and FRP bars. *Journal of Materials in Civil Engineering*, 18(6), pp.831-841.